

doi:10.3788/gzxb20184706.0630002

α -蒎稀光电离和离解动力学的同步辐射研究

刘宪云^{1,2}, 夏丽¹, 王振亚², 张为俊²

(1 常州大学 数理学院 电子科学与技术系, 江苏 常州 213164)

(2 中科院安徽光学精密机械研究所 环境光谱研究室, 合肥 230031)

摘 要:为研究 α -蒎稀的光电离解离机制, 采用同步辐射光电离质谱, 在 7.9~15.5 eV 能量范围内研究了 α -蒎稀的紫外光电离解离, 对 α -蒎稀的电离解离能及其碎片离子的出现势进行了理论分析. 实验测得光电离效率曲线, 从光电离效率曲线中获得 α -蒎稀 $C_{10}H_{16}$ 的电离能和碎片离子 $C_9H_{13}^+$, $C_7H_{10}^+$, $C_3H_6^+$ 及 CHH_3^+ 的出现势. 用 Gaussian 03 理论方法计算了 $C_{10}H_{16}$ 和主要的光解离碎片的总能量, 用高级能量计算方法计算了 $C_{10}H_{16}$ 的电离能和部分碎片离子的出现势及主要的解离通道的解离能. 根据实验和理论计算结果, 分析了产生碎片离子的主要的解离通道. 分析表明实验测得的结果与理论计算提出的 $C_{10}H_{16}$ 的光解离通道获得的解离能符合得较好.

关键词: α -蒎稀; 光电离; 光解离; 离子出现势; 同步辐射

中图分类号: O433

文献标识码: A

文章编号: 1004-4213(2018)06-0630002-6

Photoionization and Photodissociation Study of α -pinene Using Synchrotron Radiation

LIU Xian-yun^{1,2}, XIA Li¹, WANG Zhen-ya², ZHANG Wei-jun²

(1 School of Mathematics and Physics, Changzhou University, Changzhou, Jiangsu 213164, China)

(2 Laboratory of Environment Spectroscopy, Anhui Institute of Optics and Fine Mechanics, Chinese Academy of Sciences, Hefei 230031, China)

Abstract: To explain the mechanism of ionization of the α -pinene ($C_{10}H_{16}$), the VUV dissociative photoionization of $C_{10}H_{16}$ in an energy region of 7.9~15.5 eV has been investigated with a mass-spectrometer method photoionization mass spectroscopy using synchrotron radiation, the dissociation energies and the appearance energies for its fragment ions were predicted. The ionization energy of $C_{10}H_{16}$ and appearance energies for its fragment ions, $C_9H_{13}^+$, $C_7H_{10}^+$, $C_3H_6^+$ and CH_3^+ , were determined with photoionization efficiency spectroscopy. The total energies of $C_{10}H_{16}$ and its main photofragments were calculated using Gaussian 03 program. The ionization energy of $C_{10}H_{16}$, appearance potentials for its fragment ions, and the dissociation energies to produce them were predicted using high accuracy energy model. The dissociation energies of some possible dissociation channels to produce those fragment ions were determined based on comparison of determined appearance energies and energies predicted with the Gaussian-03 calculations. According to the results, the experimental dissociation energies were in reasonable agreement with the calculated dissociation energies of proposed photodissociation channels of $C_{10}H_{16}$.

Key words: α -Pinene; Photoionization; Photodissociation; Appearance energy of ions; Synchrotron radiation

Foundation item: The Scientific Research Foundation of the Education Ministry for Returned Chinese Scholars, China (No. [2013]693), and the National Natural Science Foundation of China (No. 11404039)

First author: LIU Xian-yun (1977-), female, associate professor, PhD. degree, mainly focuses on optical electronics. Email: xyliu@cczu.edu.cn

Received: Jan.18, 2018; **Accepted:** Mar.20, 2018

<http://www.photon.ac.cn>

OCIS Codes: 340.6720; 010.1100; 300.6170

0 Introduction

The total annual global emission of biogenic hydrocarbons has been estimated between 825 and 1 150 TgCyr⁻¹ as demonstrated^[1], and has exceeded anthropogenic Volatile Organic Compounds (VOC) emissions 5 to 10-fold as demonstrated^[2-3]. Monoterpenes, of which α -pinene is one of the principal species, are emitted in substantial amounts by vegetation, terpenes account for a major fraction of non-methane hydrocarbons emitted from the terrestrial biosphere, with an estimated global emission rate on the order of 1.014 kg per year. Annual natural emissions of terpenes exceed those from anthropogenic sources on a global scale. α -pinene (35%) and β -pinene (23%) are the two most abundant terpenes in the troposphere. In the atmosphere α -pinene undergoes reactions with O₃, the OH radical or the NO₃ radical, leading to low-volatility species which partly condense on existing aerosols, thereby generating secondary organic aerosols. α -pinene plays an important role in the chemistry of the lower troposphere, and in the troposphere these organic compounds react with hydroxyl (OH) radicals, nitrate (NO₃) radicals, and ozone (O₃). These reactions may contribute to the formation of aerosols, peroxides (hydrogen peroxide and organic peroxide), carbon cycle, acid rain, and active radicals such as OH radical. This has been shown in numerous laboratory experiments as demonstrated^[4-7]. But a detailed understanding of the chemical reaction pathways leading to the production of SOA is lacking, and in general the overall yield of products detected in the particle phase is typically less than 30%. Despite for that, MEJEAN M et al^[8] have shown that no gas phase ion energetics data, either experimental or theoretical, are available for this compound in the literature except for that Al-Joboury and Turner measured the ionization energy using Photoelectron (PE) method in 1964. Still, the mechanism of VUV dissociative photoionization of α -pinene is still less understood both experimentally and theoretically.

Due to the above mentioned reasons, it is important to study the mechanism of dissociative photoionization of α -pinene both experimentally and theoretically. In order to determine Ionization Energy (IE) of α -pinene and Appearance Energies (AEs) for its fragmental ions, and to explore the mechanism for its dissociative ionization, we present a study of VUV dissociative photoionization of isoprene in the energy range of $\sim 7.9 \sim 15.5$ eV. Synchrotron radiation has been used to measure Photoionization Mass Spectroscopy (PIMS) and Photoionization Efficiency (PIE) curves. The quantum chemistry calculation is also performed using Gaussian 03 program and MP2 (full) method to obtain some photochemical parameters, and then, the mechanisms of dissociative photoionization of α -pinene will also be discussed.

1 Experiment

The Photoionization Mass Spectrometry (PIMS) measurements of α -pinene were conducted on the atomic and molecular physics beam line, using VUV synchrotron radiation obtained from the electron storage ring of National Synchrotron Radiation Laboratory in Hefei, China. The experimental apparatus was described previously elsewhere as demonstrated^[9-10]. In brief, photon energies in a region of 7.5~22.5 eV with a resolving power of 5 000 at 15.9 eV and a photon flux of $\sim 10^{12}$ photons S⁻¹ were selected with a grazing-incidence Spherical Grating Monochromator (SGM) employing a grating of 1 200 grooves mm⁻¹ and a slit width of 80 μ m. For calibration of photon energies, we used the photoionization spectrum of Ar with accuracy better than 0.002 eV. A rare-gas harmonic filter was inserted into the beam line to overcome higher-order harmonics contamination in the energy range from 7.5 to 21.5 eV. The main experimental chamber is composed of a beam source chamber, a differential chamber and an ionization chamber with a Reflectron Time-of-flight Mass Spectrometer (RTOFMS).

The sample was introduced by supersonic expansion through a continuous beam nozzle with an orifice of 70 μ m diameter from the beam source chamber into the photoionization chamber through a $\phi 1$ mm skimmer. The sample molecular beam intersected the monochromatized synchrotron radiation beam at 70 mm from the nozzle. A Reflectron Time-of-flight Mass Spectrometer (RTOFMS) was employed for the VUV photoionization/fragmentation studies. Photoions produced by the VUV light were drawn out of the photoionization region by a pulse generator (DG 535 SRS) and detected by a Microchannel Plate (MCP)

detector. The ion signal was recorded by a multiscaler P7888 (FAST Comtec, Germany) after being amplified with preamplifier VT120C (EG & G, ORTEC). To normalize the ion signals, we monitored the photon intensity simultaneously with a silicon photodiode (SXUV-100, International Radiation Detectors, Inc.).

(-)- α -Pinene (purity $\geq 99.0\%$) was obtained from Fluka, Sigma-Aldrich Co., United States, and was used without additional purification in the experiment. In the experiment, we used Ar (purity 99.99%) as the carrier gas and the stagnation pressure was in the range of 1-3 bars. Ar was also used as gas filter medium and the pressure of the gas chamber is 600 Pa. Before the experiments, the pressure of the ionization chamber was about 5.1×10^{-5} Pa, and it was 3.0×10^{-3} Pa when the sample was introduced into the ionization chamber. The PIE curves was measured while the monochromator is scanned with a wavelength increment of 30 meV and the data acquisition time for each point is 30~40 s depending on ion abundance. No cluster was observed under this condition, so no fragment ions were considered to originate from cluster dissociation.

2 Theoretical calculations

The study of quantum chemical calculation of α -Pinene was performed by using Gaussian-03 program as demonstrated (Frisch et al, 2004). The equilibrium geometry and harmonic vibrational frequencies of α -Pinene are calculated using 6-31G (d,P) basis sets at B3LYP hybrid density functional level of theory as demonstrated [11-12], scaled uniformly by 0.9736. The single point energy of α -Pinene and its fragment products were calculated using 6-31G (d) basis sets with MP2 (full) method. After the calculation of the energy E_0 (MP2), the high accuracy energy model was used to calculate the thermochemical parameters, such as, ionization energy of α -Pinene, appearance energy for its fragment ions and dissociation energy to produce them.

3 Results and discussion

3.1 Results of experiment

The PIMS from the photoionization of α -Pinene measured at the photon energy of 15.5 eV is shown in Fig.1. As can be seen from the figure, the signal of the parent ion $C_{10}H_{16}^+$ is not very strong, however, the signal of fragment ion mass-to-charge ratio $m/z = 93$ is the strongest one among all fragment ions. As no signal at mass greater than that of $C_{10}H_{17}^+$ is detected under our experimental conditions, all detected fragment ions were considered to originate from dissociation of parent ion.

In order to study the SRVUV dissociative photoionization of $C_{10}H_{16}$, the Photoionization Efficiency (PIE) curves of $C_{10}H_{16}^+$ and those of the observed fragment ions, such as $C_9H_{13}^+$, $C_7H_9^+$, $C_2H_4^+$, and CH_3^+ , from their respective appearance onsets to 15.5 eV, were recorded at a scan step of 30 meV and normalized with respect to the photon flux. The PIE curves near the threshold region of the parent molecular ion $C_{10}H_{16}^+$ and some of its fragment ions, $C_9H_{13}^+$, $C_7H_9^+$, $C_2H_4^+$, and CH_3^+ , are shown in Fig.2 and 3, serve to determine the IE of $C_{10}H_{16}^+$ and AE of each fragment ion. In the study of VUV dissociative

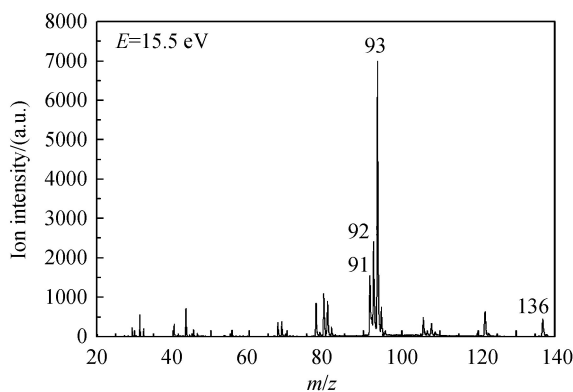


Fig.1 Photoionization mass spectra of $C_{10}H_{16}$ excited at 15.5 eV of photon energy

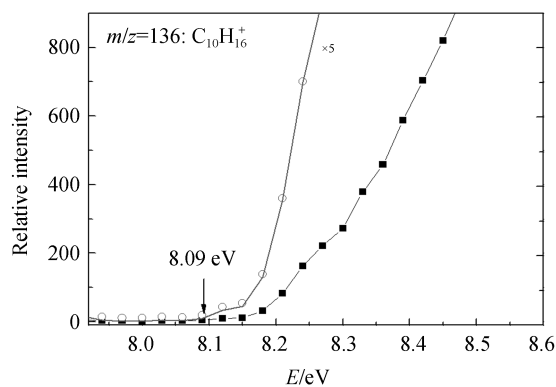


Fig.2 PIE spectra of $C_{10}H_{16}^+$

photoionization of $C_{10}H_{16}$ in the energy region 7.9~15.5 eV, the IE of $C_{10}H_{16}$ and the AEs of its fragment ions can be reached directly by scanning the photon energy of the monochromatized SR. It should be pointed out that we ignored the thermal energy distribution of the parent molecule in our data processing, considering the present nozzle expansion was made for possible kinetic shifts in determining the AEs.

In the PIE curve of $C_{10}H_{16}^+$ (cf. Fig.2), the onset of ionization of $C_{10}H_{16}$ is 8.09 ± 0.003 eV. For fragment ions, we used two approaches to determine their Appearance Energies (AE) as demonstrated [13]. For ion signals that increase linearly with ionization energy, the AE was determined from the intersection of the baseline (dot-line) and the gradually rising line (circle-line), as shown in Fig.2 for $C_{10}H_{16}^+$. When the ion signals rise abruptly but with a gradual, slow slope near the threshold, as shown in Fig.3, the AE was determined as the midpoint of the two intersects among the baseline, the slowly rising line and the rapidly rising line.

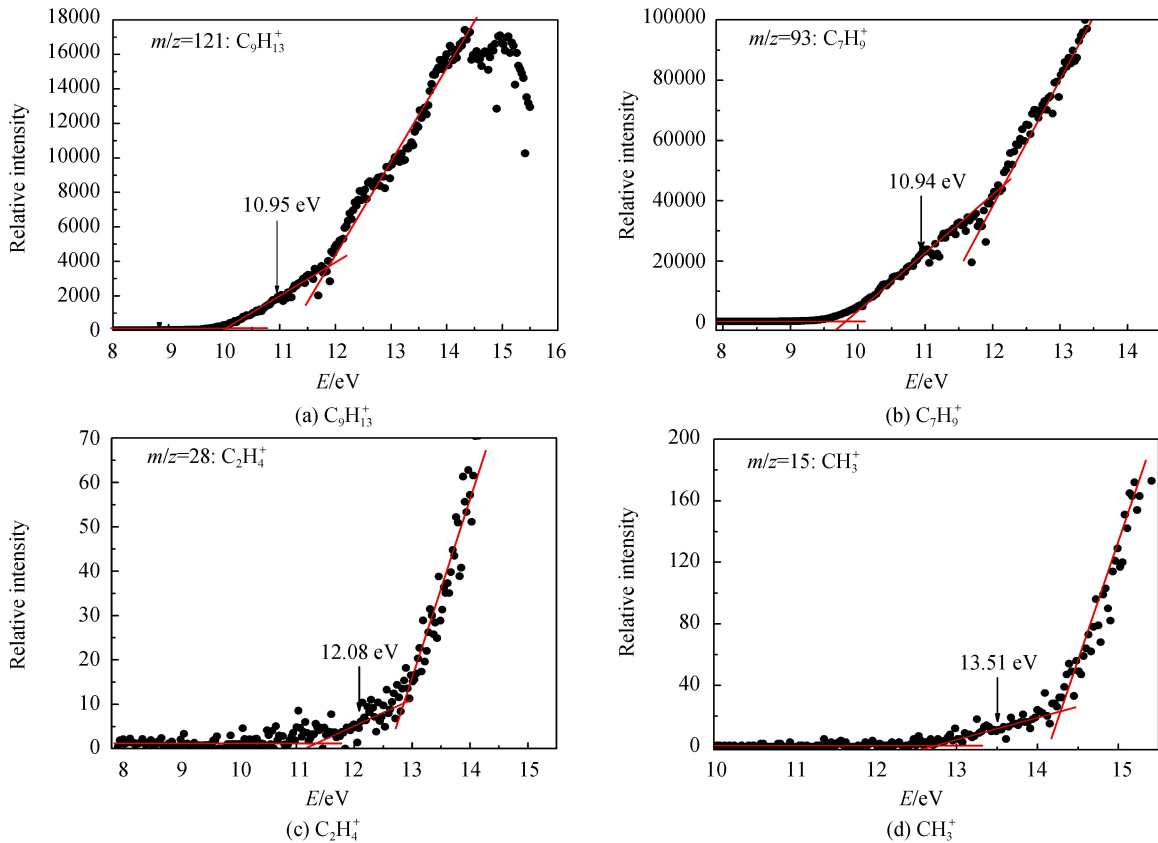


Fig.3 Photoionization efficiency curves

3.2 The dissociation channels

The dissociation channels for α -pinene producing fragment ions can be deduced in Table 1, and two possible cases should be considered during the calculation of dissociation energy: 1) The fragment ion is formed from a neutral fragment of parent molecule, and the dissociation energy is calculated by subtracting ionization energy of neutral fragment from its appearance potential; 2) The fragment ion is formed by ionization of a parent molecule followed by spontaneous dissociation of the primary parent ion as demonstrated[14]. The latter is generally referred to as dissociative ionization and the emphasis of this paper is placed on it. The dissociation energy E_d is calculated empirically by subtracting ionization energy of parent molecule from its appearance energy as follows

$$E_d = A_E - E_I$$

where E_d is the dissociation energy, A_E is the appearance energy for fragment ion, E_I is the ionization energy of parent molecule. As an example, the E_I of $C_{10}H_{16}$ is 8.09 ± 0.003 eV, the A_E of $C_9H_{13}^+$ is 8.85 ± 0.03 eV, and therefore the $E_d(C_9H_{13}^+ - CH_3)$ is 0.76 ± 0.06 eV. The E_I of $C_{10}H_{16}$ and A_E s for its fragment ions $C_9H_{13}^+$, $C_7H_9^+$, $C_2H_4^+$, and CH_3^+ , are listed in Table 1, along with some dissociation energies and possible dissociation channels of $C_{10}H_{16}$.

Table 1 Experimental, theoretical and literature values of the ionization energy, appearance energy and dissociation energy of α -pinene

Ions	E_1 or A_E DFT(B3LYP)/eV	E_1 or A_E (Exp.)/eV	E_1 or A_E (literature)/eV	Possible dissociation channels	E_d MP2(full)/eV	E_d (Exp.)/eV
$C_{10}H_{16}^+$	7.92	8.09 ± 0.003	$8.07^{[15]}$	—	—	—
$C_9H_{13}^+$	11.62	10.95 ± 0.03	—	$C_9H_{13}^+ + CH_3$	0.76	0.76 ± 0.06
$C_7H_9^+$	10.67	10.94 ± 0.03	—	$C_7H_9^+ + C_2H_4$	2.75	2.85 ± 0.06
$C_2H_4^+$	10.65	12.08 ± 0.03	—	$C_2H_4^+ + C_7H_9$	2.73	3.99 ± 0.06
CH_3^+	12.90	13.51 ± 0.03	—	$CH_3^+ + C_9H_{13}$	4.98	5.42 ± 0.06

3.3 Results of calculation

α -Pinene has two enantiomers, (S)-(-)- α -pinene and (R)-(+)- α -pinene, respectively, both enantiomers are known in nature. In this quantum chemical calculations, the (-)- α -Pinene was selected. The equilibrium properties of $C_{10}H_{16}$ was investigated using B3LYP hybrid density functional in conjunction with the 6-31G(d, p) basis sets as implemented in the Gaussian 03. The vibrational frequencies of $C_{10}H_{16}$ were calculated by the geometry optimizations as described above. Seventy-two frequencies were calculated for the *s*-trans structure of α -pinene, indicating a true minimum on the potential energy surface. In the similar way, the equilibrium properties and vibrational frequencies of $C_{10}H_{16}^+$ were also calculated using DFT B3LYP/6-31G (d, p). The formula of the species involved in this work, along with the calculated MP2 (full) energies are summarized in Table 2. With the aid of these results, we have established the dissociation channels of α -pinene.

Furthermore, we also optimized equilibrium structure of some transition structure and intermediate, calculated their total energies E_0 (MP2(full)), the MP2(full) energies E_0 (in hartrees) of various species involved in the dissociation of MBO are calculated as shown in Table 2. In high accuracy energy model of Gaussian-03, ionization energy (E_1) of each molecule is taken as the amount of energy required to remove an electron from a molecule, computed as the energy difference between the cation and the neutral molecule. For example, the theoretical ionization energy of α -pinene is calculated as follows

$$E_1(C_{10}H_{16}^+) = E_0(C_{10}H_{16}^+) - E_0(C_{10}H_{16}) = -390.471 - (-390.762) = 0.291 \text{ (Hartree)} \approx 7.92 \text{ (eV)}$$

This theoretical value of adiabatic ionization energy of α -pinene is close to our experimental one of 8.09 ± 0.003 eV.

For possible dissociation channel $C_{10}H_{16} \rightarrow C_9H_{13}^+ + CH_3$, the appearance energy (A_E) of $C_9H_{13}^+$ is calculated as

$$A_E = E_0(\text{MP2})(C_9H_{13}^+) + E_0(\text{MP2})(CH_3) - E_0(\text{MP2})(C_{10}H_{16})$$

In the dissociation channel $C_{10}H_{16} \rightarrow C_9H_{13}^+ + CH_3$, its dissociation energy is calculated as follows

$$E_d = E_0(\text{MP2})(C_9H_{13}^+) + E_0(\text{MP2})(CH_3) - E_0(\text{MP2})(C_{10}H_{16}^+)$$

Table 2 The MP2 (full) energies E_0 (in hartrees) of various species involved in the dissociation of MBO

Species	E_0 (MP2) (Hartree)	Species	E_0 (MP2) (Hartree)
$C_{10}H_{16}$	-390.762 068 05	$C_{10}H_{16}^+$	-390.470 991 21
C_9H_{13}	-350.747 777 99	$C_9H_{13}^+$	-350.479 871 64
C_7H_9	-271.059 924 95	$C_7H_9^+$	-195.436 676
CH_3	-39.855 187 78	CH_3^+	-39.491 472 13
C_2H_4	-78.509 300	$C_2H_4^+$	-78.501 087

The appearance energies of other fragment ions and some dissociation energies of other possible dissociation channels can also be calculated in similar ways. IE of α -pinene, AEs for fragmental ions, $C_{10}H_{16}^+$, $C_9H_{13}^+$, $C_7H_9^+$, CH_3^+ , and $C_2H_4^+$, as well as the E_d s of some possible dissociation channels, predicted by MP2(full) calculations, are given in Table 1. Table 1 shows that the experimental dissociation energies were in reasonable agreement with the calculated dissociation energies of proposed photodissociation channels of $C_{10}H_{16}$, but the dissociation energies to produce $C_2H_4^+$ is different, which may indicate that we should consider not only the thermo-chemistry parameters predicted using high accuracy energy model, but also some different transition states with specific barriers as demonstrated^[16].

4 Conclusion

The VUV dissociative photoionization of $C_{10}H_{16}$ has been investigated with a mass-spectrometer method PIMS using SR. The IE of $C_{10}H_{16}$ and appearance energies for its fragment ions, $C_9H_{13}^+$, $C_7H_{10}^+$, $C_3H_6^+$ and CH_3^+ , were determined with PIES. The dissociation energies of some possible dissociation channels to produce those fragment ions were determined based on comparison of determined appearance energies and energies predicted with the Gaussian-03 calculations. Results show that the experimental dissociation energies were in reasonable agreement with the calculated dissociation energies of proposed photo-dissociation channels of $C_{10}H_{16}$.

References

- [1] FEHSENFELD F, CALVERT J, FALL R, *et al.* Emissions of volatile organic compounds from vegetation and the implications for atmospheric chemistry[J]. *Global Biogeochemical Cycles*, 1992, **6**(4): 389-430.
- [2] GELENCSE'R A. Carbonaceous aerosol[M]. Springer; Dordrecht, the Netherlands, 2004; 289.
- [3] KANAKIDOU M, SEINFELD J H, PANDIS S N, *et al.* Organic aerosol and global climate modelling: A review [J]. *Atmospheric Chemistry and Physics*, 2005, **5**(4): 1053-1123.
- [4] FRATTINI L, ISAACS M A, PARLETT C M A, *et al.* Support enhanced alpha-pinene isomerization over HPW/SBA-15[J]. *Applied Catalysis B-Environmental*, 2017, **100**(1): 10-18.
- [5] SHILLING J E, CHEN Q, KING S M, *et al.* Particle mass yield in secondary organic aerosol formed by the dark ozonolysis of α -pinene[J]. *Atmospheric Chemistry and Physics*, 2008, **8**(7): 2073-2088.
- [6] ZHAO J, ORTEGA J, CHEN M, MCMURRY P H. Dependence of particle nucleation and growth on high molecular weight gas phase products during ozonolysis of α -pinene[J]. *Atmospheric Chemistry and Physics*, 2013, **13** (15): 7631-7644.
- [7] FLORES-HOLGUÍN N, AGUILAR-ELGUÉZABAL A, RODRIGUEZ-VALDEZ L M, *et al.* Theoretical study of chemical reactivity of the main species in the α -pinene isomerization reaction[J]. *Journal of Molecular Structure: Theochem*, 2008, **854**(1 - 3): 81-88
- [8] MEJEAN M, GIULIANI A, BRUNELLE A. Determination of ionization energies of a monoterpene series by atmospheric pressure photoionization using tunable vacuum ultraviolet synchrotron radiation[J]. *European Journal of Mass Spectrometry*, 2014, **20**(5): 403-407.
- [9] KONG R H, SHAN X B, WANG S S, *et al.* Experimental and theoretical study of $Ne \cdot CO$ cluster[J]. *Journal of Electron Spectroscopy and Related Phenomena*, 2007, **160**: 49-53.
- [10] WANG S S, KONG R H, SHAN X B, *et al.* Performance of the atomic and molecular physics beamline at the national synchrotron radiation laboratory[J]. *Journal of Synchrotron Radiation*, 2006, **13**(6): 415-420.
- [11] STEPHENSP J, DEVLIN F J, CHABALOWSKI C F, *et al.* Ab initio calculation of vibrational absorption and circular dichroism spectra using density functional force fields[J]. *Journal of Physical Chemistry*, 1994, **98** (45): 11623-11627.
- [12] BECKE A D. Density-functional thermochemistry. III. The role of exact exchange[J]. *Journal of Chemical Physics*, 1993, **98** (7): 5648-5652.
- [13] CHIANG S Y, BAHOU M, SANKARAN K, *et al.* Dissociative photoionization of CH_2Cl_2 and enthalpy of formation of $CHCl^+$: Experiments and calculations[J]. *Journal of Chemical Physics*, 2003, **118**(1), 62-69.
- [14] WANG Z Y, HAO L Q, ZHOU S K, *et al.* VUV dissociative photoionization of CHF_2Cl [J]. *Journal of Molecular Structure*, 2007, **826**(2-3): 192-197.
- [15] ALJOBOURY M I, TURNER D W. Molecular photoelectron spectroscopy. Part II. A summary of ionization potentials [J]. *Journal of the Chemical Society*, 1964, 4434-4441.
- [16] LIU X Y, ZHANG W J, WANG Z Y, *et al.* Dissociative photoionization of isoprene: experiments and calculations[J]. *Journal of Mass Spectrometry*, 2009, **44**(3): 404-409.

引用格式: LIU Xian-yun, XIA Li, WANG Zhen-ya, *et al.* Photoionization and Photodissociation Study of α -pinene Using Synchrotron Radiation[J]. *Acta Photonica Sinica*, 2018, **47**(6): 0630002

刘宪云, 夏丽, 王振亚, 等. α -蒎烯稀光电离和解离动力学的同步辐射研究[J]. 光子学报, 2018, **47**(6): 0630002